Fast Power Spectrum Estimation with Sparse Learning for Wideband Spectrum Sensing

Shuai Liu(✉), Wen Xiao, Yao Zhang, Jing He, and Jixin Wu

Xi'an Jiaotong University, Xi'an 710049, China
sh_liu@mail.xjtu.edu.cn

Abstract. The Compressed Sensing technology in wideband spectrum sensing (WSS) has greatly improved the utilization of spectrum resources. Based on this, we combining sparse learning and fast power spectrum estimation to achieve WSS in this paper. Sparsity adaptive matching pursuit (SAMP) algorithm is exploited to obtain the sparse sample representation for WSS. Then the limitations of power spectrum estimation in WSS are considered. To ease the limitations, the computational tasks are decomposed by multiple fast Fourier transforms. Theoretical performance analysis is made to further explain the proposed method. By improving the process of sample collection and power spectrum estimation, the proposed method can effectively achieve the pur-pose of fastly and exactly sensing. The final simulation results are utilized to verify the applicability of the proposed method and its advantages over other methods.

Keywords: Wideband spectrum sensing · Power spectrum estimation · Sparse learning

1 Introduction

In recent years, 5G technology has become more and more important in many new applications and use cases, the emergence of 5G technology puts forward higher requirements for the number of wireless device connections, which makes us have to pay attention to the effective utilization of spectrum resources. As we all know, its development is restricted by the scarcity of spectrum resources, so there is an urgent need to resolve the resource shortage by effectively utilizing the spectrum resource. WSS enables cognitive radio to be applied to a wider frequency band to meet the development of modern wireless communication. Specifically, WSS is a process which scans a wide frequency band consisting of several sub-bands of narrow frequency band, so as to find the spectral cavity in the whole bandwidth and improve the spectrum utilization. Now WSS is generally known and has become a field of interest for many researchers [1, 2]. As an important research method in WSS, CS can reduce the sampling burden and realize efficient and fast wideband spectrum sensing.

At present, there are two kinds of WSS technologies. One is the method based on Nyquist sampling [3, 4]. Pei et al. proposed the sequential scanning method in [3] which identifies the sensing order and sensing-access strategies to achieve maximum energy efficiency. In [4], filter banks are introduced as a tool in CR systems, which can achieve for spectrum sensing by choosing the proper one from various filter banks. Its

H. Gao et al. (Eds.): ChinaCom 2020, LNICST 352, pp. 421–433, 2021.
https://doi.org/10.1007/978-3-030-67720-6_29

performance is evaluated theoretically and through numerical examples. But the methods based on Nyquist sampling usually suffer from either long sensing latency or enormous hardware complexity.

Another one based on sub-Nyquist sampling is proposed [5, 6]. Among these, more and more researchers achieve the WSS by exploring the compressed sensing theory [7–12] to sense a wide frequency band via a low sampling rate. Utilizing the sparse or statistical characteristics, the wideband spectrum signals can be reconstructed at a lower sampling rate than the Nyquist rate. In [10], Zhao et al. schedules the sequential compressed spectrum sensing by jointly exploring compressed sensing and sequential periodic detection techniques to achieve more accurate and timely wideband sensing. Using the heterogeneous wideband spectrum, the latent block-like structure is exploited to construct efficient compressive spectrum sensing models for obtaining the well heterogeneous wideband spectrum in [11]. Fast matching pursuit, a fast and accurate greedy recovery algorithm, is proposed for compressed wideband spectrum sensing in [12].

However, these compressed wideband spectrum sensing approaches also suffer several limitations, including noise, the unavoidably high computational complexity of reconstruction, and the low signal-to-noise ratio.

To solve these problems, reconstructing the power spectrum of the wideband spectrum signal is proposed to replace the original signal, by using sub-Nyquist [13–15]. The feature-based method is proposed for the primary user's spectrum identification by exploring the interference immunity with a reduced amount of data in [14]. The approach in [15] exploited the statistical structure of random processes to obtain the effective signal compression and showed an alternative perspective for sparsity-agnostic inference.

In this paper, we reconstruct the power spectrum of the wideband signal through the sub-Nyquist sampling, which is achieved by exploring the sparsity of the wideband spectrum signal. Firstly, the proposed method uses the sparsity adaptive matching pursuit algorithm (SAMP) to collect signals sparsely and reserve the latent information contained in the original signal as much as possible [16, 17]. Secondly, the fast Fourier transform (FFT) is exploited to obtain a fast power spectrum estimation [18]. In this way, compared to the existing method, the proposed method can improve the computational efficiency of power spectrum reconstruction and can be effectively applied to the field of compressed wideband spectrum sensing.

2 Algorithm Design

2.1 The Proposed Method

The details of the proposed method are shown in Fig. 1. In this part, we will introduce the sample collection by using the sparse sampling method and give a detailed derivation process of how to realize the power spectrum estimation of signals with FFT, includes using FFT to decompose computing tasks to reduce computational complexity.

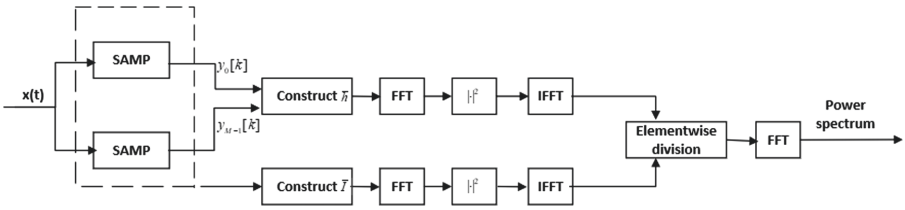

Fig. 1. The proposed method.

First of all, some samples of l moment are collected in the m th channel by using SAMP sparse sampling, it is given by

$$y_m(l) = x(lNT) \tag{1}$$

Then, since the collected data $\{y_m[l]\}_{m=1,\,l=0}^{M,\,L-1}$ is a partial subset of sub-Nyquist sampled data $\{x[n]\}_{n=0}^{LN-1}$. In order to establish the relationship between the Nyquist sampling and the sub-Nyquist sampling data, an indicator sequence $\{I[n]\}_{n=0}^{LN-1}$ and a data sequence $\{h[n]\}_{n=0}^{LN-1}$ are defined as follows

$$h[n] = \begin{cases} y_m(l), & n = lN \\ 0, & otherwise \end{cases} \tag{2}$$

$$I[n] = \begin{cases} 1, & n = lN \\ 0, & otherwise \end{cases} \tag{3}$$

In power spectrum estimation, the widely-used unbiased estimation of the signal $x[n]$ is given as

$$r_x[k] \approx \frac{1}{|\mathbf{Q}_k|} \sum_{n \in \mathbf{Q}_k} (x[n]x^*[n-k]) \tag{4}$$

where $\mathrm{Q}_k = \{n | 0 \le n-k \le LN-1, 0 \le n \le LN-1\}$, Only data $\{\mathrm{h}[n]\}$ can be obtained in the experiment, so we get a new unbiased estimation which is computed by

$$\begin{aligned} r_x[k] &\approx \frac{1}{Q_k} \sum_{n \in \hat{\mathbf{Q}}_k} (x[n]x^*[n-k]) \\ &= \frac{1}{Q_k} \sum_{n \in \mathbf{Q}_k} (h[n]h^*[n-k]) \end{aligned} \tag{5}$$

where

$$Q_k \triangleq \left|\hat{\mathbf{Q}}_k\right| \triangleq \{n|I[n]I[n-k]=1\} \tag{6}$$

once $\{r_x[k]\}$ is calculated, the power spectrum can be calculated by DFT.

In order to improve the spectrum resolution, L should be as large as possible within the allowable range, but in this way, it will significantly increase the computational complexity. Therefore, FFT is introduced in the solution process to solve this problem. we divide (5) into two parts and introduced FFT for calculation respectively.

The first part can be defined as

$$r_h[k] = \sum_{n=0}^{LN-1} (h[n]h^*[n-k]) \tag{7}$$

where $n<0$ or $n \geq LN$, let $h[n]=0$. At this point, we define $\left\{\hat{h}[n]\right\}_{n=-LN+1}^{LN-1}$ to be the reverse for $\left\{\overline{h}[n]\right\}_{n=-LN+1}^{LN-1}$ and define $\left\{\overline{h}[n]\right\}_{n=-LN+1}^{LN-1}$ as follows

$$\overline{h}[n] = \begin{cases} h[n], & LN-1 \geq n \geq 0 \\ 0, & -LN+1 \leq n < 0 \end{cases} \tag{8}$$

Then $r_h[k]$ can be written as

$$\begin{aligned} r_h[k] &= \begin{cases} \sum_{n=-LN+1+k}^{LN-1} (\bar{h}[n]\hat{h}^*[k-n]), k \geq 0 \\ \sum_{n=-LN+1}^{LN-1+k} (\bar{h}[n]\hat{h}^*[k-n]), k<0 \end{cases} \\ &\overset{(a)}{=} \sum_{n=-LN-1}^{LN-1} (\bar{h}[n]\hat{h}_P^*[k-n]) \\ &= (\bar{h} * \hat{h}^*)[k] \end{aligned} \tag{9}$$

where $P \triangleq 2NL-1$. As the periodic sum of $\hat{h}[n]$,$\hat{h}_P[n]$ can be shown as

$$\hat{h}_P[n] \triangleq \sum_{k=-\infty}^{+\infty} \hat{h}[n-kP] \tag{10}$$

The symbol * of (9) represents cyclic convolution, and (a) represents: When $-LN+1 \leq n<0$,$\overline{h}[n]=0$ and when $-2LN+1 \leq n<-LN$, $\hat{h}_P[n]=\hat{h}[n-NL]=0$. From this We can get as follows

$$\begin{aligned} r_h &\triangleq [r_h[-LN+1]...r_h[LN-1]]^T, \\ \bar{h} &\triangleq [\bar{h}[-LN+1]...\bar{h}[LN-1]]^T, \\ \hat{h} &\triangleq [\hat{h}[-LN+1]...\hat{h}[LN-1]]^T. \end{aligned} \tag{11}$$

By referring to the theorem of circular convolution, it can be obtained: $F_{2NL-1}r_h = (F_{2NL-1}\bar{h}) \circ (F_{2NL-1}\hat{h})$. F_{2NL-1} represents the discrete Fourier Transform (DFT) at (2NL − 1)-point. ∘ represents the product of corresponding elements in two vectors. Since $\{\hat{h}[n]\}$ represents the time reversal for $\{\bar{h}[n]\}$, consider the property of complex-conjugate and time-reversal for DFT, the sequence $\{\hat{h}^*[n]\}$ is the DFT complex conjugate of $\{\bar{h}[n]\}$. So we can get

$$(F_{2NL-1}\bar{h}) \circ (F_{2NL-1}\hat{h}) = \left|F_{2NL-1}\bar{h}\right|^2 \tag{12}$$

Where $|\bullet|^2$ represents the square of the complex vector module. Finally, we can get the final form of r_h shown as

$$r_h = F_{2NL-1}^{-1}\left|F_{2NL-1}\bar{h}\right|^2 \tag{13}$$

According to (6), the second part is defined as:

$$Q_k = \sum_{n \in \mathbf{Q}_k} I[n]I[n-k] \tag{14}$$

At this point, we calculate Q_k by introducing FFT, firstly, we define

$$\begin{aligned} q &\triangleq [Q_{-LN+1} \cdots Q_{LN-1}]^T, \\ \bar{I} &\triangleq [\bar{I}[-LN+1] \ldots \bar{I}[LN-1]]^T. \end{aligned} \tag{15}$$

where

$$\bar{I}[n] = \begin{cases} I[n], & LN-1 \geq n \geq 0 \\ 0, & -LN+1 \leq n < 0 \end{cases} \tag{16}$$

Note that the definition of the second part is similar to the first part, according to the computational process of (7), we can get $q = F_{2NL-1}^{-1}\left|F_{2NL-1}^{-1}\bar{I}\right|^2$.

After we compute $\{Q_k\}$ and $\{r_h[k]\}$, we get the result of (5): $r_x[k] = r_h[k]/Q_k$. The final power spectrum estimation can be obtained by performing DFT on this result.

2.2 Theoretical Performance Analysis

We found that the proposed method only involves FFT, IFFT and some simple multiplication operations. It can be easily calculated through floating-point operations in total. Obviously, compared with existing methods, the proposed method is dominant in the calculation and can compute efficiently in parallel. In this part, we will calculate the mean square error (MSE) for the proposed method, and make a theoretical analysis of it.

$\hat{s}$ represents the estimated power spectrum, and s represents the actual power spectrum. MSE can be solved as

$$\begin{aligned} \mathrm{E}[\|\hat{s}-s\|_2^2] &\overset{(a)}{=} \|\mathrm{E}[r_x]\|_2^2 + 1^T \mathrm{D}(r_x) - 2\mathrm{E}[\hat{s}]^H s + \|s\|_2^2 \\ &= \|\mathrm{E}[\hat{s}] - s\|_2^2 + 1^T \mathrm{D}(r_x) \end{aligned} \tag{17}$$

In (17), r_x represents the autocorrelation vector estimation, F represents the DFT matrix, and (a) represents: $\mathrm{E}[\|r_x\|_2^2] = \|\mathrm{E}[r_x]\|_2^2 + 1^T \mathrm{D}(r_x)$, 1 is a vector where all terms are 1, $\mathrm{D}(r_x)$ is the variance of each element for r_x. Therefore, the mean square error of the estimator can be given by

$$\mathrm{MSE} = 1^T \mathrm{D}(r_x) \tag{18}$$

we simplify the main calculation task to the variance of the r_x element of the vector, therefore, we obtain

$$\begin{aligned} &\mathrm{D}(r_x[k]) \\ &= \mathrm{E}\left[\left| \frac{1}{Q_k^2} \sum_{n \in \mathbf{Q}_k, m \in \mathbf{Q}_k} (x[n]x^*[n-k]x[m]x^*[m-k]) \right|^2 \right] - |\mathrm{E}[r_x[k]]|^2 \end{aligned} \tag{19}$$

we assume a special case where the signal $x[t]$ is a white signal with zero mean and variance σ^2. When $k \neq 0$, there is $\mathrm{D}(r_x[k]) = \frac{1}{Q_k^2}\sigma^4$; Where $k = 0$, $\mathrm{D}(r_x[k]) = \frac{\sigma^4}{Q_0^2}$. Therefore, for this special case, MSE can be simplified as

$$\mathrm{MSE} = 1^T \mathrm{D}(r_x[k]) = \sigma^4 \sum_k 1/Q_k \tag{20}$$

It is easy to conclude that the increase in the number of data samples will reduce MSE, while the more sparse learning sampling data, the larger $\{Q_k\}$ can be obtained, thus estimating accurately.

3 Simulation Experiments

In this part, this paper provides experimental results to prove the accuracy and effectiveness of the proposed method.

3.1 The Setting of Experimental Parameters

During the experiment, this paper uses the band-pass FIR filter to filter zero-unit variance White Gaussian Noise and produces 5 wide-sense stationary signals in the frequency range of [0, 1] GHz. The purpose of this experiment is to identify the frequency position of the signal propagating over the band [0, 1] GHz. For the system parameters, we set the signal component bandwidth as 10 MHz, and 2 GHz for the

Nyquist sampling rate, the carrier frequencies are set as 100, 210, 360, 450, and 670 MHz respectively. SAMP algorithm is adopted to collect the sub-Nyquist samples in this proposed method, so we set the number of sampling channels as M = 8, the sampling rate as 100 MHz in each channel, and we collect the samples with a duration of 1 ms for each channel in this experiment. The downsampling factor is set as $N = fnyq/(100MHz) = 20$. The spectral resolution is set to 60 kHz, corresponding to the 33,335-length power spectrum. Therefore, there is $2NL \geq 33335$, and $L \geq 32000/2N \approx 667$ data samples need to be collected for each sampling channel. Finally, we consider the selection of window function, which can reduce the spectrum energy leakage. We use a hanning window to the autocorrelation sequence in this proposed method, in order to achieve a more accurate power spectrum estimation.

3.2 The Analysis of Experimental Results

First, we design an experiment with the results shown in Fig. 2. The signal-to-noise ratio (SNR) is set as −5 dB in each experiment. Zero mean Gaussian noise is used to corrode the original signal to generate noise signals. Here, SNR is given as

$$\mathrm{SNR} = 10\log_{10}\frac{\sum_{n=1}^{N_t}|x[n]|^2}{N_t\sigma^2} \tag{21}$$

It can be seen from Fig. 2 that the proposed method can recover the true power spectrum accurately. In addition, the results show that for the sub-Nyquist sampling data within 10 ms, the recovery accuracy of the proposed method is slightly higher than the condition of 1 ms samples. The results show that the accuracy of power spectrum estimation with sparse learning can be improved by increasing the sampling time.

Figure 3 shows the ROC curve of the method proposed in this paper with different SNRs, this advantage is particularly suitable for WSS, the receiver must work in a low SNR state to obtain sensitivity in the practical sense, it can be calculated as

$$S = 10\log(kT_{syst}) + 10\log(B) + NF_{RX} + SNR \tag{22}$$

In (22), B represents the bandwidth of the signal, NF_{RX} means the noise figure of the receiver, and its value is 6 dB. Therefore, we can calculate the receiver sensitivity is $S = -174\mathrm{dBm/Hz} + 10\log(1\mathrm{GHz}) + 6\mathrm{dB} + \mathrm{SNR} = -78\mathrm{dBm}$. In order to achieve the receiver sensitivity of −80 dbm, in this case, we take the SNR as $-80 - (-78) = -2\,\mathrm{dB}$. The sampling rate of ADC is set as 100 MHz, 125 MHz, and 200 MHz respectively. The corresponding downsampling factor n are 20, 16, and 10, respectively. As we can see, the result of Fig. 4 is based on the condition that SNR is set as −15 dB. Figure 4 shows that the performance of the method is gradually improved with the increase of the sampling rate.

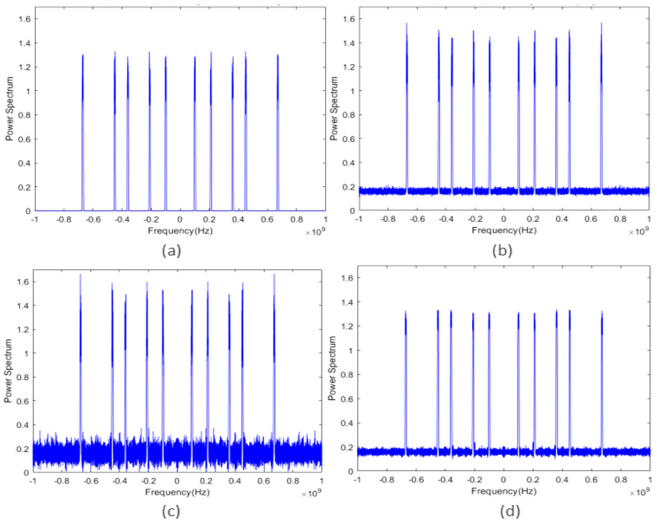

Fig. 2. The results of power spectrum reconstruction with different samples and method: (a) noiseless Nyquist samples collected within 1 ms; (b) noisy Nyquist samples collected within 1 ms;(c) 1 ms noise sub-Nyquist samples via the proposed method; (d) 10 ms sub-Nyquist samples via the proposed method.

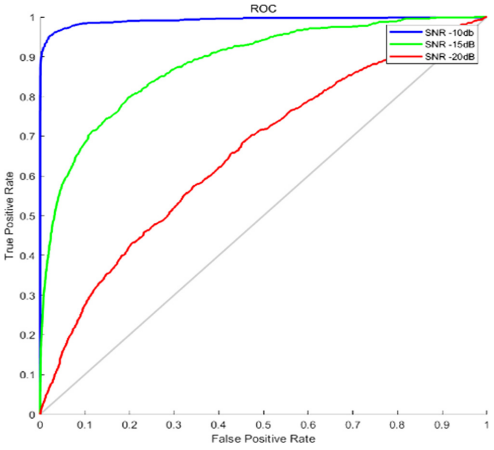

Fig. 3. True positive rate and false positive rate in different SNRs.

From the running time of the experiment shown in Fig. 5, it can be seen that the proposed method significantly improves the computational efficiency compared with the frequency-domain method. We find that there is the same number of channels and sampling rate for MWC and SAMP algorithms, so the comparison is reasonable. For these two methods, though collecting data samples at an interval of 1 ms, this experiment considers that the frequency resolution is set as 62.5 kHz. The operating

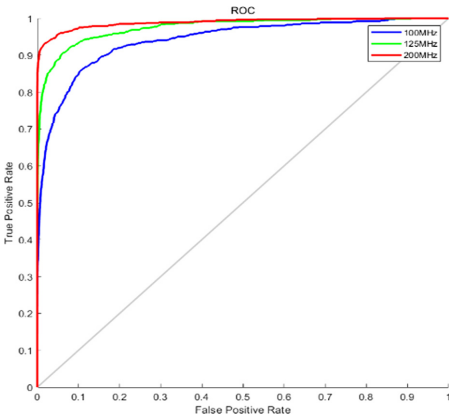

Fig. 4. True positive rate and false positive rate in different compression ratios.

conditions of the experiment are as follows: a 2.60 GHz Intel i7CPU and 16.0 GB of RAM laptop using MATLAB R2020a. The average running time and ROC curves are showed in Fig. 5, which can be seen that our method attains convergence faster than the frequency- domain method. In addition, the time required by the proposed method is about half of that of the frequency-domain method, therefore, we can conclude, our method effectively reduces the computational complexity, the practical system based on FPGA can be better implemented [19].

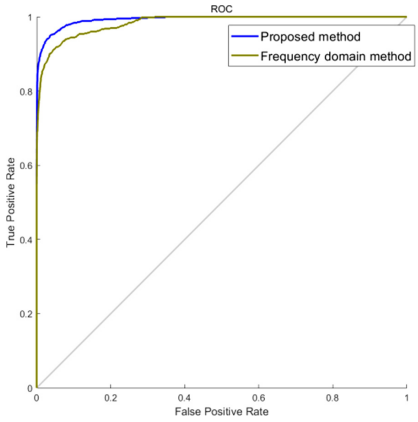

Fig. 5. The ROC of the frequency-domain method and our method, the running times are 0.36 s and 0.18, respectively.

We also set a experiment based on the assumption that the time-domain method uses sparse learning [20], to compare the proposed method with the traditional time-domain method [21], its results are shown in Fig. 6. The values of some system

parameters are the same as those described above. Specially, we set the SNR as −12 dB, and the frequency resolution as 1 MHz. Data samples continuously collected within 0.1 ms were used in this experiment. Figure 6 shows the ROC curve and the average running time of this experiment. As we can see from the experimental results in Fig. 6, the proposed method has better performance than the traditional time-domain method.

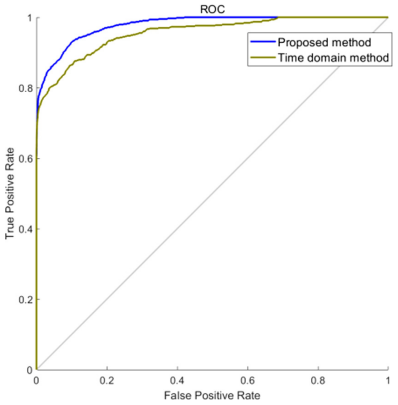

Fig. 6. The ROC of the proposed method and the time-domain method, the running times are 0.03 s and 0.13 s, respectively.

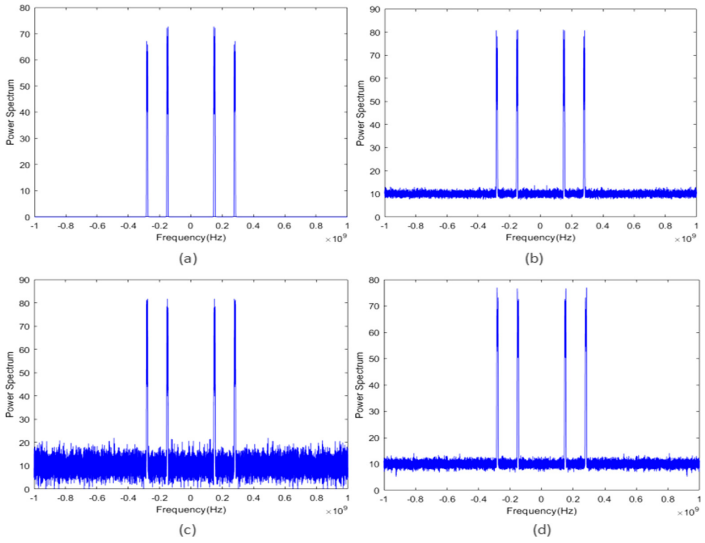

Fig. 7. The results of power spectrum reconstruction with different samples and method: (a) 1 ms noiseless Nyquist samples; (b)1 ms noisy Nyquist samples; (c) 1 ms noise sub-Nyquist samples, under the proposed method; (d) 10 ms sub-Nyquist samples, under the proposed method.

The proposed method is based on the assumption that multi-band signals are generalized stationary, and the generalized stationarity is a widely used assumption for spectrum sensing, also for compressed power spectrum estimation [22]. However, the actual signal may be either cyclostationary or non-stationary. The statistical properties of non-stationary random signals, such as mean and variance, vary with time. In other words, it is characterized by slow time-varying statistics. So they can be regarded as generalized stationery signals for a short time in these circumstances, and the proposed method is also suitable for cyclostationary communication signals. In order to prove these results, we simulate two cyclostationary communication signals, QAM16 signal and BPSK signal whose frequency range is [0, 1] GHz, The carrier frequencies are set as 280 MHz and 150 MHz respectively, the SNR is set as −10 dB, and the sparse learning sampling architecture is set as mentioned earlier in this section. From Fig. 7, we can conclude that the proposed method is suitable for cyclostationary signals and can produce accurate power spectrum estimation for it.

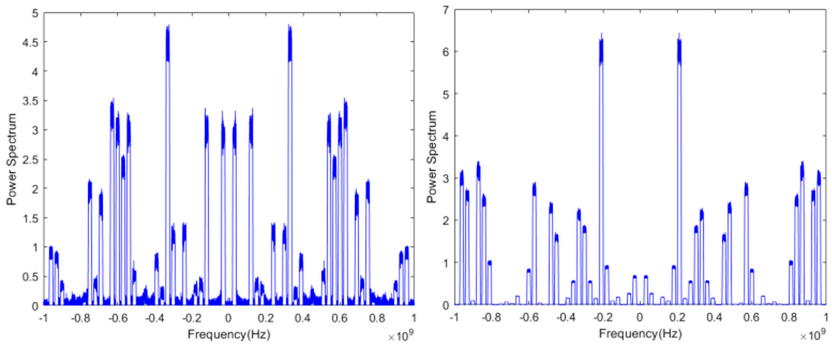

Fig. 8. Left: Reconstruct the power spectrum using 10 ms noiseless Nyquist samples under the proposed method; Right: Reconstruct the power spectrum using noiseless Nyquist samples collected within 1 ms.

In order to illustrate that the method proposed in this paper does not impose a sparse constraint on the monitored spectrum when reconstructing the power spectrum [23], we carried out this experiment in a multiband signal consisting of 32 narrowband components in a frequency range of [0, 1] GHz and set the bandwidth of narrowband signal as 20 MHz. The spectrum occupancy is computed as (32 × 20 MHz)/(1 GHz) = 64% from the parameter settings described earlier, it shows that the monitored power spectrum is not sparse. Two comparative experiments are shown in Fig. 8. In the results of the reconstructed power spectrum showed in Fig. 8, we set the NMSE as 0.0014 and 0.0055 respectively. As we can see, this method also provides a precise power spectrum estimation even if the monitored spectrum is not sparse.

4 Conclusion

In this paper, we introduce the sparse sampling method and FFT into the fast power spectrum estimation. Aiming at the high computational complexity of traditional methods and unable to meet the requirements of the real-time spectrum sensing system, a fast compressed power spectrum estimation method is proposed. By collecting the sub-Nyquist samples with sparse sampling, we improve the sampling rate in WSS. Next, the method reconstructs the power spectrum estimation model, specially, when L is large, it will provide better spectral resolution, but increase the computational complexity in this model. To address the problem, FFT is introduced into the computational process, the computational complexity is reduced by using three FFT. Experimental data analysis shows that the proposed method can meet the requirements of a real-time spectrum sensing system with low computational complexity and can be effectively implemented in the actual system, the final experimental results listed above also prove the effectiveness and computational efficiency of our method.

Acknowledgement. This research was funded by the National Natural Science Foundation of China (No. 61703328), the China Postdoctoral Science Foundation funded project (No. 2018M631165), the Fundamental Research Funds for the Central Universities (No. XJJ2018254).

References

1. Sun, H., Nallanathan, A., Wang, C.X., Chen, Y.: Wideband spectrum sensing for cognitive radio networks: a survey. IEEE Wirel. Commun. Mag. **20**(2), 74–81 (2013)
2. Ali, A., Hamouda, W.: Advances on spectrum sensing for cognitive radio networks: theory and applications. IEEE Commun. Surv. Tutorials **19**(2), 1277–1304 (2017)
3. Pei, Y., Liang, Y.C., The, K.C., Li, K.H.: Energy-efficient design of sequential channel sensing in cognitive radio networks: optimal sensing strategy, power allocation, and sensing order. IEEE J. Sel. Areas Commun. **29**, 1648–1659 (2011)
4. Farhang-Boroujeny, B.: Filter bank spectrum sensing for cognitive radios. IEEE Trans. Signal Process. **56**, 1801–1811 (2008)
5. Zhao, Y., Chen, Y., Zheng, Y.: Wideband power spectrum estimation based on sub-nyquist sampling in cognitive radio networks. IEEE Access **7**, 115339–115347 (2019)
6. Shaban, M., Perkins, D., Bayoumi, M.: Application of compressed sensing in wideband cognitive radios when sparsity is unknown. In: 15th IEEE Wireless and Microwave Technology Conference (2014)
7. Donoho, D.L.: Compressed sensing. IEEE Trans. Inf. Theory **52**(4), 1289–1306 (2006)
8. Laska, J., Wen, Z., Yin, W., Baraniuk, R.: Trust, but verify: fast and accurate signal recovery from 1-bit compressive measurements. IEEE Trans. Signal Process. **59**(11), 5289–5301 (2011)
9. Khalfi, B., Hamdaoui, B., Guizani, M., Zorba, N.: Efficient spectrum availability information recovery for wideband DSA networks: a weighted compressive sampling approach. IEEE Trans. Wirel. Commun. **17**, 2162–2172 (2018)
10. Li, Z., Xu, W., Zhang, X., Lin, J.: A survey on one-bit compressed sensing: Theory and applications. Front. Comput. Sci. **12**(2), 217–230 (2018)
11. Peng, X., Bin, L., Xiaodong, H., Quan, Z.: 1-bit compressive sensing with an improved algorithm based on fixed-point continuation. Sig. Process. **154**, 168–173 (2019)

12. Zhang, X., Du, H., Qiu, B., Chen, S.: Fast sparsity adaptive multipath matching pursuit for compressed sensing problems. J. Electron. Imaging **26**(3), 033007 (2017)
13. Cohen, D., Eldar, Y.C.: Sub-Nyquist sampling for power spectrum sensing in cognitive radios: a unified approach. IEEE Trans. Signal Process. **62**, 3897–3910 (2014)
14. Lagunas, E., Nájar, M.: Spectral feature detection with sub-Nyquist sampling for wideband spectrum sensing. IEEE Trans. Wirel. Commun. **14**, 3978–3990 (2015)
15. Romero, D., Arianandа, D.D., Tian, Z., Leus, G.: Compressive covariance sensing: structure-based compressive sensing beyond sparsity. IEEE Sig. Process. Mag. **33**, 78–93 (2016)
16. Liquan, Z., Ke, M., Yanfei, J.: Improved generalized sparsity adaptive mathching pursuit algortithm based on compressive sensing. J. Electr. Comput. Eng. (2020)
17. Khobahi, S., Soltanalian, M.: Signal recovery from 1-bit quantized noisy samples via adaptive thresholding. In: 52nd Asilomar Conference on Signals, Systems, and Computers (2018)
18. Kumar, A., Saha, S.: FFT-based multiband spectrum sensing in SIMO in-band full-duplex cognitive radio networks. Radio Sci. **55**(6) (2020)
19. Wang, P., You, F., He, S., Zhao, C.: A double screening orthogonal-matching-pursuit algorithm for compressed sensing receiver with high column correlation sensing matrix. IEICE Electron. Express **16**(18) (2019)
20. Eldafrawy, M., Boutros, A., Yazdanshenas, S., Betz, V.: FPGA logic block architectures for efficient deep learning inference. ACM Trans. Reconfigurable Technol. Syst. **13**(3), 1–34 (2020)
21. Manohar, C., Halaki, A., Gurugopinath, S.: Cooperative spectrum sensing based on flatness in spectral domain under noise variance uncertainty
22. Beck, E., Bockelmann, C., Dekorsy, A.: Compressed edge spectrum sensing: extensions and practical considerations. at-Automatisierungstechnik **67**(1), 51–59 (2019)
23. Wang, Y., Pandharipande, A., Polo, Y.L., Leus, G.: Distributed compressive wide-band spectrum sensing. In: Information Theory and Applications Workshop, pp. 178–183. IEEE (2009)